JOURNAL OF MATERIALS SCIENCE 11 (1976) 1385–1392

The tensile deformation behaviour of a transparent ABS polymer

R. W. TRUSS, G. A. CHADWICK
Department of Mining and Metallurgical Engineering, University of Queensland, St. Lucia, Queensland 4068, Australia

A transparent ABS polymer has been tested in uni-axial tension over a range of strain rates. The effect of strain rate on the yield stress has been explored and the magnitude of the activation volume obtained. By simultaneously monitoring volume strain and longitudinal strain, the contribution of crazing to the total deformation has been derived and shown to vary with strain rate. A detailed optical and electron microscopy study of the crazing and fracture behaviour of this material has also been conducted.

1. Introduction

In previous work, we studied the deformation of pigmented ABS polymers, examining the variations with strain rate of yield stress and the contribution of crazing to the post yield deformation [1]. It was found that at a strain rate of 1.4×10^{-1} sec^{-1}, all the deformation was associated with crazing while at lower strain rates, only approximately 25 to 50% could be attributed to crazing. The present work was undertaken on a transparent ABS material which behaved in a similar fashion to the pigmented ABS but which allowed the deformation and crazing to be directly observed and readily studied both macroscopically and microscopically.

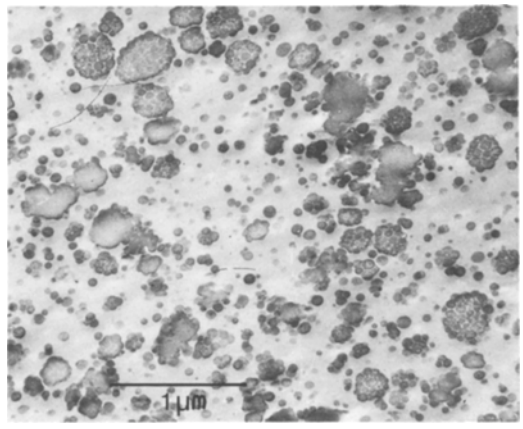

Figure 1 Transmission electron micrograph of osmium stained Cycolac C.I.T. brand ABS.

2. Experimental

2.1. Material

The material used in this work was Cycolac CIT brand transparent ABS polymer supplied by Marbon Chemical Pty. Ltd. The microstructure of this material was determined in the electron microscope using specimens prepared by Kato's technique in which the elastomer particles were hardened and stained with OsO_4 allowing ultrathin sections to be prepared by microtomy [2]. Fig. 1 shows that the rubber particles range in size from roughly 500 to 7500 Å, and that the larger particles have a distinctly composite structure. The smaller particles also show some internal structure.

The material was in the form of injection moulded tensile test bars having a shape specified by B.S. 2782 having a parallel gauge length of 50.8 mm with a cross-section 12.7 mm by 3.2 mm. All specimens were annealed at approximately 80° C for 2 h before testing.

2.2. Procedures

Tensile tests were conducted at room temperature over a range of strain rates to determine the effect of strain rate on the yield stress. An Instron testing machine was used at constant cross-head speeds ranging from 0.5 to 500 mm min^{-1}. The machine

was considered hard with respect to the specimen and strain rates were calculated from the crosshead speed. This gave strain rates of approximately 10^{-4} to 10^{-1} sec^{-1}.

The contributions of crazing and shear deformation to the longitudinal strain were determined by adopting the postulate of Bucknall and Clayton that shear deformation occurs at constant volume so that all volume strain results from crazing [3]. The contribution of crazing is then given by the slope of a volume strain versus longitudinal strain plot. The volume strain during tensile tests was monitored using a displacement method described in a previous paper [1].

Specimens deformed at the different strain rates were then studied under the optical microscope. Specimens for transmission microscopy were thinned by the normal metallographic technique of abrasion using a light pressure on successive grades of emery paper flooded with water. Transverse and longitudinal sections of the gauge length to be examined under oblique reflected light were prepared using a similar method. When necessary, the final polish was on a Silvo wheel. Microsections and fracture surfaces for electron microscopy were coated with aluminium by vapour deposition and studied in the scanning mode.

3. Results

3.1. General observations

For all strain rates used, the load extension curve obtained for this material was similar to that described previously for other grades of ABS [1]. At the lowest strain rate of 1.4×10^{-4} sec^{-1}, crazing nucleated slightly before the general yield point both internally and near the surface and large numbers of these crazes continued to nucleate and grow up to $\simeq 5$ mm in length through the yield point. As the strain increased, the gauge length became more and more heavily whitened as smaller crazes and general stress whitening developed between the tips of the large crazes and over the whole bar.

The number of crazes present varied with the batch of material used. Of the two batches used, one displayed a huge number of crazes (Fig. 2a), while the other exhibited a much smaller number which were associated with a larger amount of general whitening. At higher strain rates, this variation between batches was not as marked.

At a strain rate of 1.4×10^{-3} sec^{-1}, large numbers of small crazes nucleated just before the yield point. These were associated with a general whitening of the bar which often appears as oblique zones between the crazes (Fig. 2b). A distinct neck formed during the post yield drop in load and this necked region was heavily stress whitened. At the still higher strain rate of 1.4×10^{-1} sec^{-1}, general stress whitening appeared over the whole gauge length near the yield point and no distinct large crazes could be seen (Fig. 2c).

In all cases, fracture occurred perpendicular to the applied load in a heavily stress whitened region

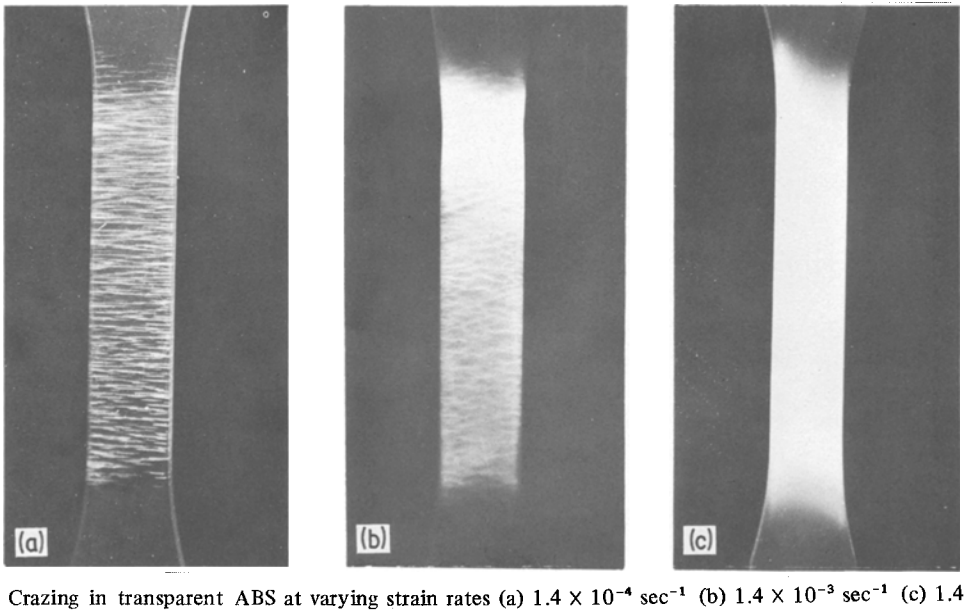

Figure 2 Crazing in transparent ABS at varying strain rates (a) 1.4×10^{-4} sec^{-1} (b) 1.4×10^{-3} sec^{-1} (c) 1.4×10^{-1} sec^{-1}.

of the gauge length. In many cases, the crack was seen to propagate slowly before the specimen failed catastrophically.

3.2. Optical microscopy

To further study the change in the crazing behaviour of this material with strain rate, specimens were tested at the different strain rates to approximately 12 to 15% strain. The gauge length was then thinned and examined in transmitted light under the optical microscope. Fig. 3a shows the typical structure obtained with the slowest strain rate used (1.4×10^{-4} sec^{-1}) and the batch of material where relatively few large crazes formed. (Note that in transmitted light the normal contrast effects are reversed). There are two different whitening patterns present and these are drawn in Fig. 4. The first (Fig. 4a) seen at A in Fig. 3a shows bands of stress whitening appearing at the tips of the craze at approximately 33° to the plane of the craze and an elliptical region centred on the craze that is relatively free of stress whitening. This type of structure is typical also of the second batch of material where a large number of the large crazes formed. The second (Fig. 4b) is seen at B where a fan shaped region of unwhitened material spreads out from the centre of the craze at about 45° to the plane of the craze while the bands at the tip of the craze remain. In some cases, a small crack could be seen at the focus of these regions. In all cases at higher magnifications, the whitened regions appeared as much smaller non-planar crazes.

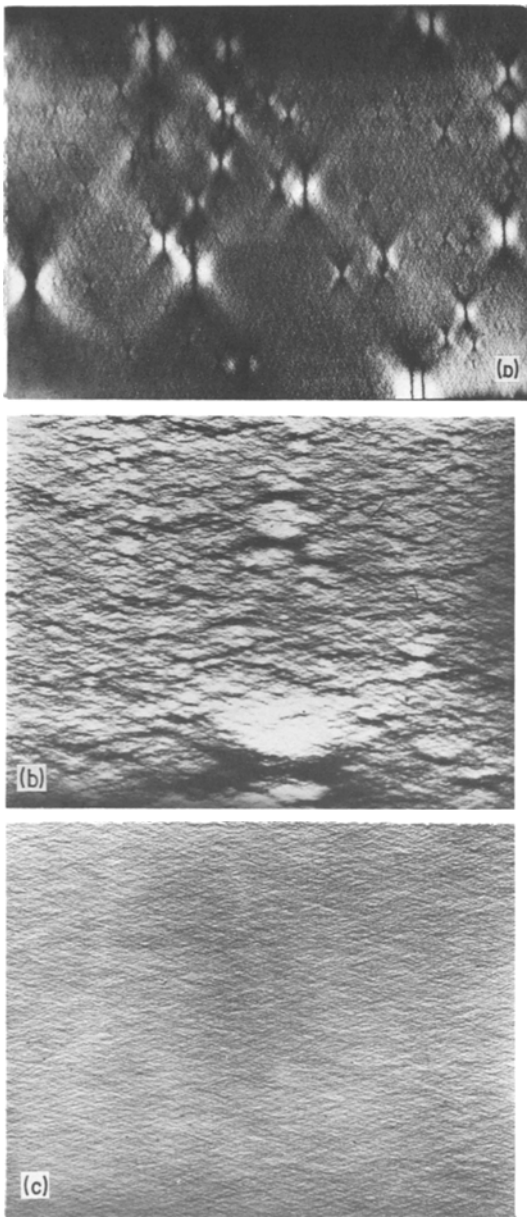

Figure 3 Transmission optical micrographs of crazing in transparent ABS at varying strain rates (a) 1.4×10^{-4} sec^{-1} (b) 1.4×10^{-2} sec^{-1} (c) 1.4×10^{-1} sec^{-1}. × 6.

As the strain rate increases, the size of the crazes becomes progressively smaller. Fig. 3b shows the craze structure formed at a strain rate of 1.4×10^{-2} sec^{-1}. Few large crazes have formed and those which have are associated with a large number of smaller crazes on planes neighbouring the plane of the major craze and there is some indication of a pattern similar to that drawn in Fig. 4a. At the highest strain rate used (1.4×10^{-1} sec^{-1}), the stress whitening consisted of a huge number of small non-planar crazes with no large crazes present (Fig. 3c). At higher magnification, these crazes often appeared like stringlets of voids.

To study the shape of the large crazes formed at slow strain rates, transverse sections of the specimens tested at a strain rate of 1.4×10^{-4} sec^{-1} were prepared and examined under oblique reflected light. It can be seen from Fig. 5 that crazes nucleated all along the centre line of the bar, the smaller crazes being circular in cross section (Fig. 6) and the larger crazes elliptical (Fig. 7). When the crazes were growing on the same or closely parallel planes, their growth was mutually arrested producing structures similar to that seen at A in Fig. 5. The crazes generally did not strike the surface of the bar; this is likely to have been due to a surface layer effect resulting from the injection moulding.

In all of the crazes, river lines were observed

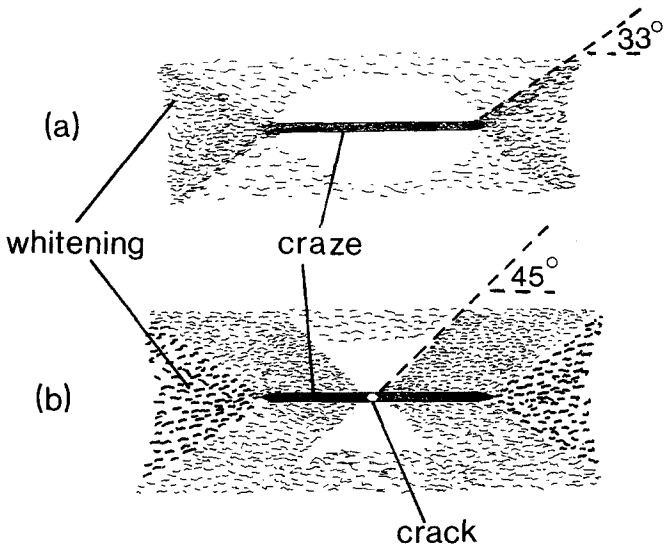

Figure 4 Stress whitening patterns around crazes formed at a strain rate of 1.4×10^{-4} sec^{-1}.

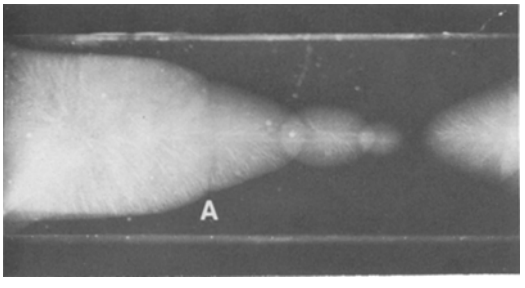

Figure 5 Transverse section of crazes formed at a strain rate of 1.4×10^{-4} sec^{-1} observed under oblique reflected light. × 7.

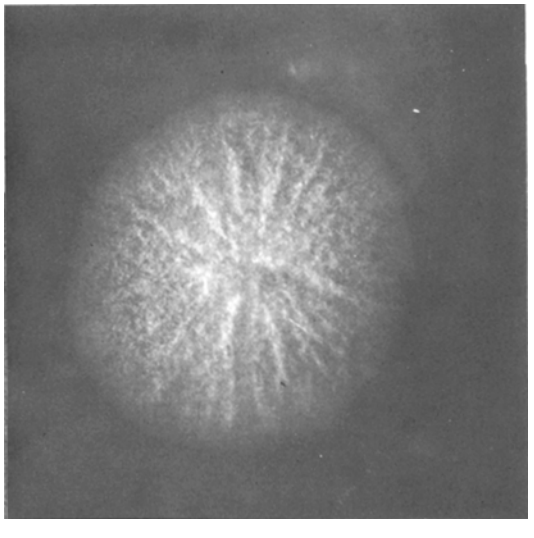

Figure 6 Transverse section of a smaller circular craze formed at a strain rate of 1.4×10^{-4} sec^{-1} observed under oblique reflected light. × 70.

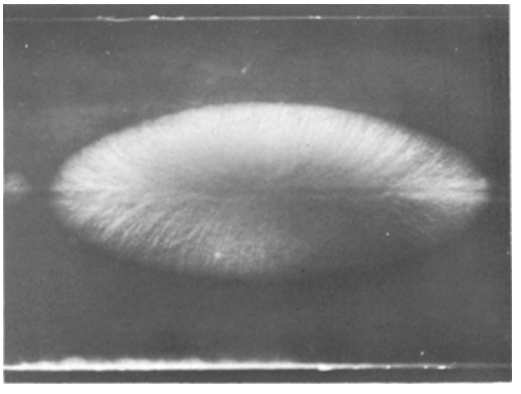

Figure 7 Transverse section of an elliptical craze formed at a strain rate of 1.4×10^{-4} sec^{-1} observed under oblique reflected light. × 14.

radiating out from the centre of the craze. When the surface layer of the specimen was removed so that the crazes intersected the new surface, the plane of the craze appeared to vary slightly, such variations being consistent with the presence of river lines in the craze as seen under oblique illumination.

3.3. Yield point effects and volume strain measurements

The Eyring rate equation

$$\dot{e} = A \exp \frac{-(\Delta H - \sigma v)}{kT} \qquad (1)$$

where $\dot{e}$ is the strain rate, σ the applied stress, v the activation volume, T the absolute temperature and k and A constants has been found to describe the

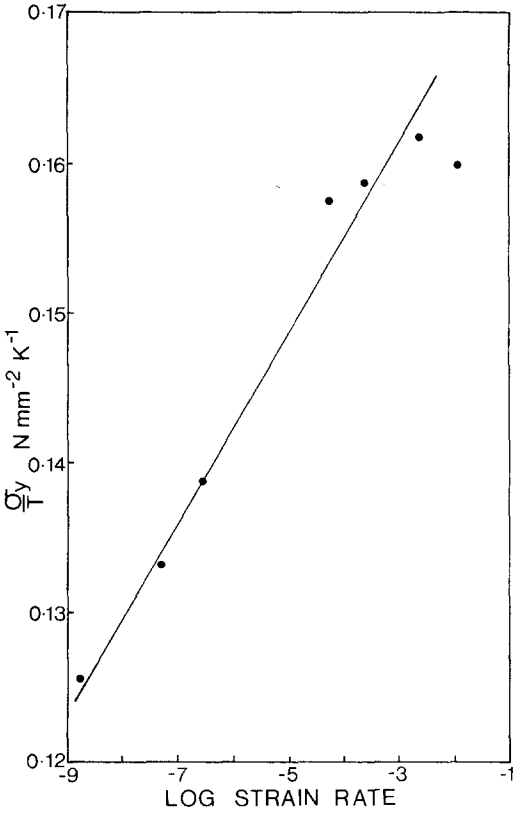

Figure 8 Graph of yield stress versus strain rate for transparent ABS at room temperature.

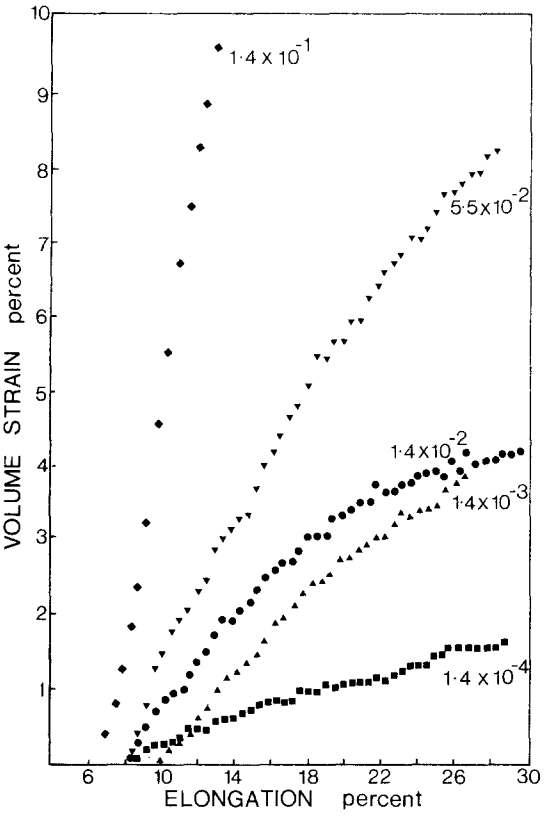

Figure 9 Relationship between volume strain and longitudinal strain at different strain rates for transparent ABS at room temperature.

yield point variation with strain rate and temperature for other grades of ABS [1]. A plot of σ_y/T versus $\dot{\epsilon}$ for this material is shown in Fig. 8 from which the value of the activation volume was calculated as 2200 Å^3. This compares with the values reported earlier of 2300 Å^3 and 3200 Å^3 for pigmented ABS with a low and high molecular weight matrix [1].

Fig. 9 shows plots of volume strain ($\Delta v/v\%$) against longitudinal strain ($\Delta l/l\%$) for different strain rates, the gradient of the plots giving an estimate of the contributions of crazing and shear deformation. As the longitudinal strain increases, the contribution of crazing to the deformation decreases except for the high strain rate of 1.4×10^{-1} sec^{-1} where crazing contributes all of the deformation. The approximate slopes of the early part of these plots are given in Table I. It can be seen that as the strain rate increases the initial rate of crazing increases moderately at low strain rates but more than doubling between 5.5×10^{-2} sec^{-1} and 1.4×10^{-1} sec^{-1}.

Two samples were tested in the volume strain apparatus to around the yield point at a strain rate

TABLE I Approximate initial slopes of the volume strain versus longitudinal strain plots at different strain rates at room temperature

Strain rate	Approximate initial slope
1.4×10^{-4} sec^{-1}	0.10
1.4×10^{-3}	0.28
1.4×10^{-2}	0.30
5.5×10^{-2}	0.47
1.4×10^{-1}	1.10

of 1.4×10^{-1} sec^{-1} so that a small number of crazes were introduced into the specimen. The lengths of these crazes were measured under the microscope which allowed the planar area of craze to be estimated assuming the shapes of the crazes were similar to those shown in Fig. 5. The small crazes were taken as circular while the larger crazes were taken as elliptical having a minor axis that varied with the length of the craze. Thus a volume per unit area of craze could be calculated and the results are given in Table II. It was considered that the estimate of the area of the crazes was con-

TABLE II Estimated volume per unit area of crazes formed at a strain rate of 1.4×10^{-4} sec^{-1}

Specimen	Strain %	$\frac{\Delta V}{A}$ (mm^3 mm^{-2})
1	7.25	0.04
2	8.60	0.06

servative which would give an over estimate of volume per unit area. It can be seen, however, that there is a slight increase in volume per unit area of craze with an increase in strain which would be consistent with a slight thickening of the crazes with increasing strain.

In order to examine directly the crazes produced at this strain rate, one of the above samples was cleaved at liquid nitrogen temperature and examined under the scanning electron microscope. Fig. 10 shows a cross-section of a craze which appears, to all intents and purposes, as a line of voids across the sample. That the crazes still contain solid material is clear since the fracture pattern is continuous across the craze. These crazes are approximately 0.01 mm thick.

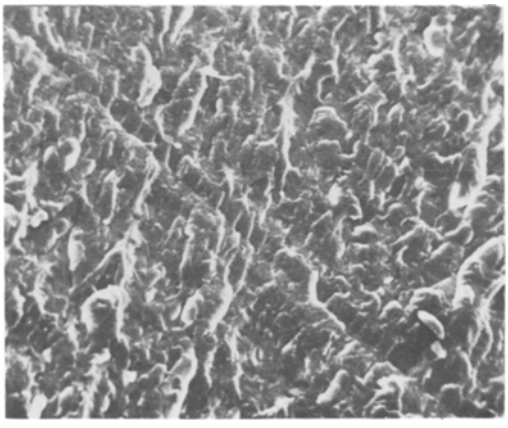

Figure 10 Scanning electron micrograph of crazed sample cleaved at liquid N_2 temperature. Specimen tested at strain rate 1.4×10^{-4} sec^{-1}. × 160.

3.4. Fracture

Fracture occurred always perpendicular to the tensile stress direction and usually in a highly stress whitened region of the gauge length. Fig. 11 shows a typical fracture surface with a concave region associated with slow crack propagation and a more rugged region where the crack propagated catastrophically. Fracture always initiated either at a surface defect or at an internal flaw, usually an inclusion, which was seen at the centre of the concave region. Lines radiating from the point of

Figure 11 Fracture surface of transparent ABS tested at a strain rate of 1.4×10^{-1} sec^{-1}. This is typical of the fracture surfaces at all strain rates used. × 15.

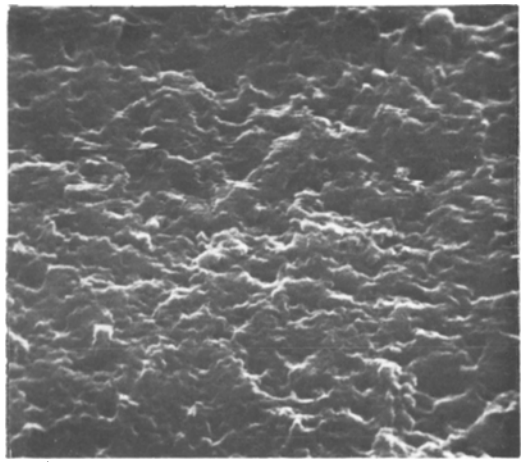

Figure 12 Highly drawn structure of the slow crack propagation region of the fracture surface. Specimen tested at a strain rate of 1.4×10^{-1} sec^{-1}. SEM. × 7200.

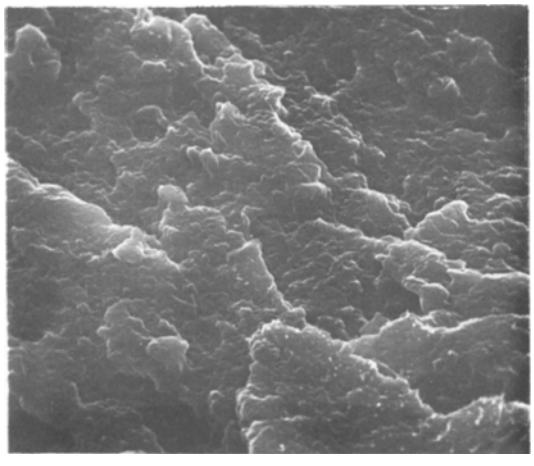

Figure 13 Structure of the fracture surface where the crack is propagating catastrophically. Specimen tested at a strain rate of 1.4×10^{-1} sec^{-1}. × 1400.

initiation were always observed in this concave region. Higher magnification of this region shows it to be highly drawn (Fig. 12). In the region where the crack was propagating catastrophically, this drawn structure was not evident and the surface was much more rugged (Fig. 13). Little difference was observed between the fracture surfaces at high and low strain rates except that at the lower strain rates several concave regions often appeared on the surface. These were frequently more highly drawn than at the higher strain rates.

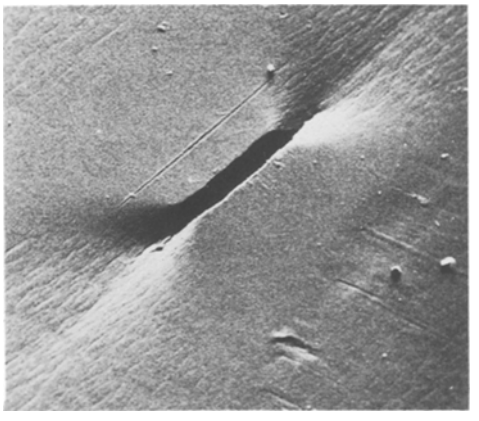

Figure 14 Crack and associated stress whitening opening up in the structure of specimen. SEM. × 70.

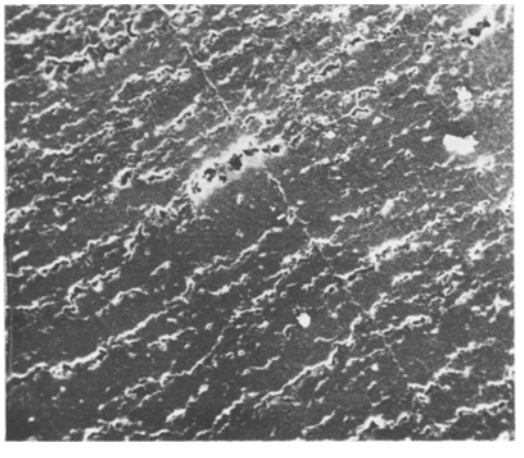

Figure 15 Voids and cracks in the tip region of a surface crack. SEM. × 1550.

Fig. 14 shows a crack opening up in the surface of a bar. Fanning out at both ends of the crack at approximately 45° are regions of smaller cracks shown in Fig. 15. These appear to be stringlets of voids running roughly perpendicular to the applied stress which are opening up and coalescing. Voiding of this type occurred wherever stress whitening struck the surface.

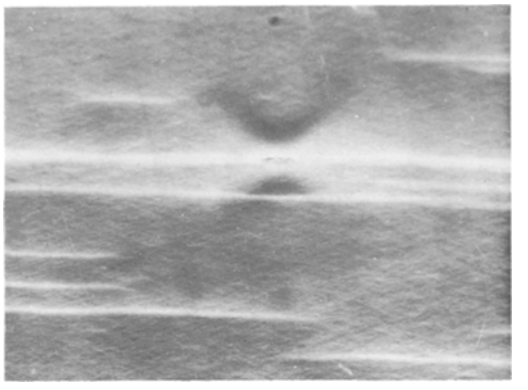

Figure 16 Crack opening up within a craze in a specimen tested at a strain rate of 1.4×10^{-4} sec^{-1}. Oblique reflected light. × 15.

To further study the fracture of this material, specimens were tested almost to fracture. The surface was then slowly ground away to reveal internal cracks. Fig. 16 shows a crack opening up within a craze in a specimen tested at 1.4×10^{-4} sec^{-1}. The crack is associated with regions of unwhitened and heavily whitened material similar to that shown in Fig. 4b. At higher strain rates, the crack was not associated with a distinct large craze but was still associated with the regions of whitened and unwhitened material observed at the lower strain rates.

4. Discussion

The yield stress variations with strain rate and the activation volume of this transparent ABS are similar to those reported earlier for other grades of ABS [1]. The variation of volume strain production and therefore crazing with strain rate also follows a similar trend to the other grades of ABS indicating that the results of the microscopy of this material may be generally applicable to other grades of ABS.

Following the established convention, the Eyring analysis was conducted on that point of the stress–strain curve where the rate of increase in load on the specimen was zero. In the light of the present results it is somewhat misleading to call this point a yield point since crazing occurs before this point is attained and therefore substantial localized plastic deformation is occurring before the load on the sample begins to drop.

Craze initiation is known to have a time–stress interdependence, the lower the applied stress or strain the longer before crazes initiate [4]. At low strain rates, the stress relaxation associated with

the formation of a large craze inhibits the build up of large internal stresses and thus limits the number of crazes nucleated. At higher strain rates, more and more sites for craze initiation are activated and with this, the size of the crazes decrease until at the highest strain rate used, a very high density of very small crazes was present.

A crack cannot support a load across it. A craze is a crack-like discontinuity in which fibrils of drawn polymer connect the two faces of the crack and therefore it is expected that a craze could support some load but less than the corresponding volume of uncrazed material. Knight [5] has calculated that the macroscopic tensile stress on the craze plane within the craze is slightly less than the applied tensile stress. However, at the tip of a craze, the stress is concentrated in a similar fashion to the stress concentration at a crack tip. An enhanced craze nucleation in the high stress regions coupled with a reduced craze nucleation in the regions of lower stress would account for the pattern of deformation shown in Fig. 4a. Fig. 4b can be considered a later stage in the deformation when a crack has nucleated within the craze. The fan like region of heavily crazed material is produced from the stress concentration at the crack tip which nucleates crazes within the region that was previously relatively uncrazed.

The results for the fracture of the clear ABS material suggest that the failure of this material is not unlike the ductile fracture of copper described by Rogers [5]. Ductile fracture of metals in tension is initiated by the formation of voids which grow and coalesce to form a crack. Shear strain concentrated at the tip of the crack opens further voids through which the crack can propagate. In the clear ABS under investigation, the initial void nucleates at an inclusion and grows by coalescing with the voids present in the crazes. At low strain rates, the crack is confined to one of the large crazes. Coalescence of the voids requires the ductile tearing of the fibres connecting the surfaces of the craze producing on the fracture surface the typical drawn structure shown in Fig. 12. At higher strain rates, no large craze was evident. Since the structure shown in Fig. 12 is typical of the fracture surfaces at all the strain rates used, the crack must propagate at the higher strain rates by growing either through many small crazes nucleated simultaneously or through a succession of small crazes formed in front of a propagating crack tip: a stress concentration at the tip of the crack nucleates crazes and opens up voids in a manner shown in Fig. 15. At a critical length, the crack propagates catastrophically by jumping between these pre-existing crazes producing the rugged structure of Fig. 13.

5. Conclusions

(1) The variation of the yield stress with strain rate and the Eyring activation volume of the clear ABS, 2200 Å, are similar to those found previously for pigmented ABS. The variation with strain rate of the contribution of crazing to the deformation of the transparent ABS also follows a similar trend to the pigmented ABS which indicates the results obtained for the clear ABS may apply more widely to the pigmented materials.

(2) The crazing behaviour of clear ABS is strain rate dependent. At a strain rate of 1.4×10^{-4} sec^{-1}, a small number of large crazes up to 5 mm in length were formed before the gauge length became heavily stress whitened. The formation of these large crazes contributed only 10 to 50% of the deformation. At higher strain rates, larger numbers of smaller crazes were formed until at a strain rate of 1.4×10^{-1} sec^{-1}, a huge number of very small crazes were formed. These small crazes often appeared non-planar. At this strain rate crazing could account for all of the deformation.

(3) The fracture of this clear ABS material initiated at an internal flaw or at a surface defect. At a strain rate of 1.4×10^{-4} sec^{-1}, the crack apparently propagated in a large craze whereas at strain rates of 1.4×10^{-1} sec^{-1} no large craze was evident but the crack propagated through a highly stress whitened region. The slow crack propagation produced highly drawn double cone fracture surfaces; when the crack propagated catastrophically the fracture surfaces appeared much more rugged.

6. References

1. R. W. TRUSS and G. A. CHADWICK, *J. Mater. Sci.* **11** (1976) 111.
2. K. KATO, *J. Electr. Mic.* **14** (1965) 220.
3. C. B. BUCKNALL and D. CLAYTON, *J. Mater. Sci.* 7 (1972) 202.
4. R. P. KAMBOUR, *Macromolecular Reviews* 7 (1973) 1.
5. A. C. KNIGHT, *J. Polym. Sci.* Part A **3** (1965) 1845.
6. H. C. ROGERS, *Trans. AIME* **218** (1960) 498.

Received 5 January and accepted 27 January 1976.